A Novel Calibration-Free Motion Sensing Technique With Single-Channel Interferometric Radars

Wei Xu, *Graduate Student Member, IEEE*, Shuqin Dong, *Graduate Student Member, IEEE*, Changzhan Gu, *Senior Member, IEEE*, and Junfa Mao, *Fellow, IEEE*

***Abstract*— Radar interferometry is widely used for detecting versatile displacement motions. The conventional techniques for motion extraction depend on the quadrature I/Q signals, and the proper calibration of the I/Q signals is a necessary step to ensure accurate motion detection. However, the calibration process and the I/Q architecture inevitably add up to the system complexity. In this article, a novel single-channel-based phase demodulation (ScPD) technique is proposed to reconstruct the precise phase information of the displacement motions, which not only employs only one single receiver channel but also eliminates the I/Q signals calibration. In addition, the proposed technique is immune to the phase ambiguity issue. To detect versatile motions with both regular and irregular patterns, approaches including envelope unwrapping, null point rejection, and outlier elimination are proposed and integrated to increase the robustness of the proposed technique. Both simulation and experiments were carried out to validate the proposed technique. The experimental results show that the proposed ScPD technique can obtain both periodic and irregular motions with high accuracy of a root mean square error (RMSE) of 0.011 mm and strong robustness to low signal-to-noise ratio (SNR) and I/Q mismatch with an RMSE of 0.015 mm. Moreover, the proposed technique is superior in detecting subtle motions, e.g., 3-μm displacement motion with an RMSE of 0.43 μm.**

***Index Terms*— Calibration free, displacement, interferometry, linear demodulation, motion sensing, radar, single channel.**

I. Introduction

INTERFEROMETRIC radar sensors are advantageous in displacement motion detection, having merits, such as noncontact, high sensitivity, and robustness against environmental interferences, such as temperature and light. Compared with other sensing strategies, such as infrared and camera, the measurement with radar interferometry is superior in long-time signal monitoring especially for the huge architecture and exhibits an outstanding adaptability to the outdoor environment [1], [2], [3], [4], [5], [6]. For example, the radar interferometry could be utilized in landslide warning by ground monitoring at full time [1]. Moreover, the interferometric sensors based on the millimeter-wave (MMW) radars have the characteristics of short wavelength, small size, and low power consumption [2], [3]. MMW radar sensor could achieve a high resolution, which is sensitive to subtle vibrations of biological tissues in clinical diagnosis. In recent years, the motion interferometry is developed for various sensing applications, such as human respiration and heartrate measurement [4], skin burn injuries diagnosis [2], structural health monitoring [5], and vehicle tracking [6].

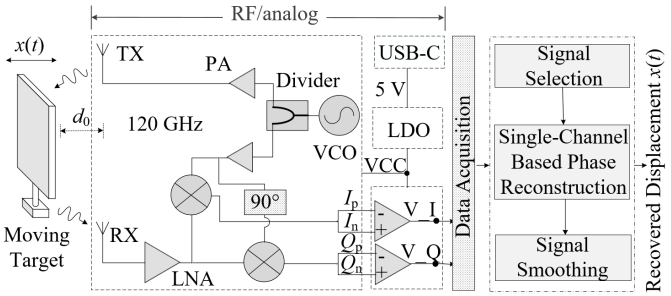

Fig. 1. Block diagram of interferometric motion sensing with the proposed ScPD technique.

As Fig. 1 shows, the motion measurement with radar interferometry succeeds based on RF hardware and signal processing. A series of electromagnetic continuous waves are generated by the signal source. A portion of the waves are radiated to the free space through the transmitting antenna (TX) and the other enter the input of mixers as local oscillation (LO) signal. When the transmitted signals meet objects in the radiation direction, part of the signals are reflected back and captured by the receiving antenna (RX). After downconversion with the LO signals, a pair of quadrature I/Q signals are output from the interferometric radar. The target motion is modulated in the phase of the backscattered signals, which could be further processed to recover the phase history representing the motion trajectory.

The conventional motion demodulation methods depend on the quadrature signals [7], [8] and the proper calibration is prerequisite for accurate motion sensing. During the calibration processing, the dc offsets and amplitudes of the I/Q signals are adjusted in terms of the phase trajectory in the constellation until the trajectory arc fits on the unit circle centered on the origin. Inaccurate calibration may result in failure of motion reconstruction. Studies show that, affected by the target surface and the nominal

Manuscript received 13 June 2022; revised 10 September 2022; accepted 16 October 2022. Date of publication 29 November 2022; date of current version 13 January 2023. This work was supported in part by the National Key Research and Development Program of China under Grant 2020YFB1807304, in part by the Natural Science Foundation of China under Grant 62171277 and Grant 61831016, and in part by the Shanghai Municipal Science and Technology Major Project under Grant 2021SHZDZX0102. This article is expanded from the work presented at 2022 IEEE International Microwave Symposium [DOI: 10.1109/LMWC.2022.3167794]. *(Corresponding author: Changzhan Gu.)*

The authors are with the MoE Key Laboratory of High-Speed Electronic Systems and the MoE Key Laboratory of Artificial Intelligence, Shanghai Jiao Tong University, Shanghai 200240, China, and also with the Shanghai AI Laboratory, Shanghai, China (e-mail: changzhan@sjtu.edu.cn).

Color versions of one or more figures in this article are available at https://doi.org/10.1109/TMTT.2022.3222422.

Digital Object Identifier 10.1109/TMTT.2022.3222422

0018-9480 © 2022 IEEE. Personal use is permitted, but republication/redistribution requires IEEE permission.
See https://www.ieee.org/publications/rights/index.html for more information.

Authorized licensed use limited to: Shanghai Jiaotong University. Downloaded on September 17,2023 at 14:27:56 UTC from IEEE Xplore. Restrictions apply.

distance to the radar, hardware defects and static clutter reflection arouse unwanted dc offsets [7], [8]. Nonlinear terms (cosine and sine terms) in the quadrature signals contain the effective dc components, which need to be compensated by calibration approaches, such as least-square (LS) algorithm [11], Levenberg–Marquardt (LM) algorithm [12], compressed sensing (CS)-based algorithm [13], and segmental phase correction [14]. Moreover, subtle motion detection and poor signal-to-noise ratio (SNR) situations may make these abovementioned phase-arc fitting methods fail to estimate the fitting center and therefore result in false demodulation, which leads to wrong reconstructed motion trajectory [15]. To solve the I/Q mismatch issue, varieties of the signal precondition methods, i.e., the ellipse compensation [16], [28], are proposed to add more orthogonality to the I/Q signals. However, the extra preconditioning may increase the complexity of the signal processing and introduce estimating errors, which would threaten the accuracy of phase recovery.

Based on the well-calibrated I/Q signals, sorts of phase demodulation algorithms are developed. The widely used arctangent method [8], [17] could unwrap the I/Q phases with several simple logical operations. However, phase discontinuity and jumping truncation may happen when the target motion displacement outstrips a quarter wavelength [18]. The higher carrier frequency is used to obtain the optimal sensing condition in recent studies. For the MMW radar, i.e., 2.5-mm wavelength for 120-GHz radar sensor, microvibration may arouse the phase ambiguity and make the phase demodulation fail. Although avoiding the codomain limitation, the differentiate and cross-multiply (DACM) algorithm [19], [20] increases the processing operations and introduces the approximate errors and accumulating noise, which weaken the accuracy of the recovered motion histories. Arcsine algorithm [21] could demodulate the I/Q phases without ambiguity, but it strengthens the requirement on the I/Q orthogonality and the SNRs of the quadrature signals.

To reduce the dependence on the I/Q signals and the calibration process, a single-channel-based phase demodulation (ScPD) technique for accurate motion interferometry is proposed by Xu et al. [22]. By the method of the signal segmentation and the Hilbert transformation, the proposed ScPD technique works with a single channel and avoids the calibration step, which effectively eliminates the false calibration introduced errors and gets rid of the dependence on the quadrature I/Q signals. Moreover, the motion reconstruction with the proposed ScPD technique shows a high tolerance to the I/Q mismatch. However, due to the codomain limitation within the 1/4 wavelength, [22] is restrained in the application of the linear motion and the periodic motion with a small displacement detection.

This article extends to improve the ScPD technique with more robustness and universality with the solutions for detecting the versatile motions with both the regular and irregular patterns. It also tackles the imperfections, such as null-point problem, low SNR, dead points, and outliers, occurring in the actual motion measurement situation. More details, such as the in-depth theory, the quantitative analysis, and comparisons with the state-of-the-art demodulation techniques, are described in this article. Thorough simulations and experimental validations are also presented.

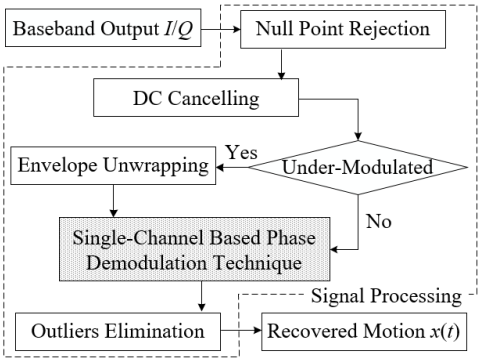

Fig. 2. Flowchart of the signal demodulation with the proposed ScPD technique. To detect the versatile motion, the proposed technique integrates several signal processing steps, including null point rejection, envelope unwrapping, and outlier elimination.

On the basis of [22], several signal processing steps including the envelope unwrapping, invalid signal rejection in null point, and outlier elimination are integrated into the ScPD technique, as illustrated in Fig. 2. Compared with [22], the ScPD technique proposed in this article not only avoids the false demodulations aroused by the improper calibrations and the I/Q mismatch but also succeeds in reconstructing the motions with various patterns. Canceling the codomain limitation, the proposed technique in this work solves the phase ambiguity issue induced by the envelope modulation, which may occur in the detection of the large displacement motions with the irregular patterns. Without the calibration step and the extra preconditions, the proposed ScPD technique reduces the complexity of the phase demodulation and recovers the target motion with high accuracy and SNR tolerance. In contrast with the conventional approaches, one signal channel with a better quality is selected from the I/Q signals before the phase demodulation with the ScPD technique by comparing the SNRs of the two output signal channels, which effectively avoids the null-point errors and achieves the reconstructed results with an intended accuracy. It is true that many commercial RF transceivers already offer integrated quadrature downconverters. However, this work may provide solid investigations and verifications for the development of future radar transceivers for motion sensing applications.

This article is organized as follows. In Section II, the basic theories and principles of the proposed ScPD technique are introduced. A series of analysis are carried out to verify the performance of the proposed ScPD technique, as shown in Section III. Section IV exhibits the experimental setup of the custom-designed 120-GHz interferometric radar sensing system with the proposed ScPD technique and experimental results of periodic motions with the modulated envelope, the I/Q mismatch, and the irregular motion detection, such as microsnapping gesture by fingers and chest-wall movement.

II. Working Principle

The dashed block in Fig. 1 illustrates a custom designed 120-GHz interferometric radar sensor, and a pair of quadrature signals modulated with target motion in the phases are output. After sampling by an analog-to-digital converter (ADC), the

Authorized licensed use limited to: Shanghai Jiaotong University. Downloaded on September 17,2023 at 14:27:56 UTC from IEEE Xplore. Restrictions apply.

raw I/Q signals could be formulated as

$$I_r(t) = A_{Ir} \cdot \cos[\theta + 4\pi (d_0 + x(t))/\lambda + \Delta\varphi] + \mathrm{DC}_{Ir} \tag{1}$$

$$Q_r(t) = A_{Qr} \cdot \sin[\theta + 4\pi (d_0 + x(t))/\lambda + \Delta\varphi] + \mathrm{DC}_{Qr} \tag{2}$$

where A_{Ir}/A_{Qr} represents the amplitude of the raw I/Q signals, respectively, d_0 is the nominal distance between the radar and the moving target, $x(t)$ is the desired displacement motion, λ is the wavelength of the LO signal, θ is the phase shift aroused by round trip of the electromagnetic signals, $\Delta\varphi$ is the residual phase noise in the circuit, and $\mathrm{DC}_{Ir}/\mathrm{DC}_{Qr}$ contains the dc offsets from the quadrature channels and the stationary clutter from the environment.

A. Single-Channel-Based Phase Demodulation

On the contrary to the conventional demodulation methods, the proposed ScPD technique reconstructs the target motion with a single receiver channel, which eliminates the dependence on the I/Q orthogonality and avoids the signal calibration process. Moreover, the proposed ScPD technique shows a high robustness to the I/Q mismatch, which means that the motion recreation with the proposed approach is immune to the imbalanced amplitudes and phases. As a result, the ScPD technique proposed in this article not only avoids the errors aroused by the false calibration but also reduces the complexity of the signal processing and the accumulating noises, which improves the accuracy and stability of the recovered motion history.

After comparing the SNRs of the I/Q signals, the signal channel in the null point could be rejected and an optimal channel is selected for further processing. By eliminating the mean power of the raw signals in (1)/(2), the selected single-channel signal could be formulated as

$$\begin{aligned} S_s(t) &= A_s \cdot \sin[\theta + 4\pi (d_0 + x(t))/\lambda + \Delta\varphi] \\ &= A_s \cdot \sin[\phi(t)] \end{aligned} \tag{3}$$

where A_s represents the amplitude of the chosen signal.

The whole process of the proposed ScPD technique is shown in Fig. 3. The selected single-channel signal is divided into a series of processing cells (S_{si}, $i = 1, 2, 3, \ldots, N$, i indexes the cell number, N is the amount of the cells) by a fixed-length sliding window. The window length should be much smaller than the period of the target motion, so the signal phase in the observing window could be modeled as a linear function of t. As shown in (3), the target displacement motion is modulated in the phase of $S_s(t)$ and the signal phase is strictly related to the carrier wavelength. According to small-angle approximation principle, if the target displacement varies within a quarter of the LO wavelength, the window-cell signal could be treated as

$$S_{si}(x(t)) \approx S_{si}(k \cdot t). \tag{4}$$

To eliminate the false transformation at the endpoint, an overlapping area ($S_{\mathrm{ol}i}$, $i = 1, 2, 3, \ldots, N-1$, the amount of the overlapping cells is less than that of segmentation units) is added between the adjacent processing cells. As (3) shows, the target displacement could be extracted from the phase of

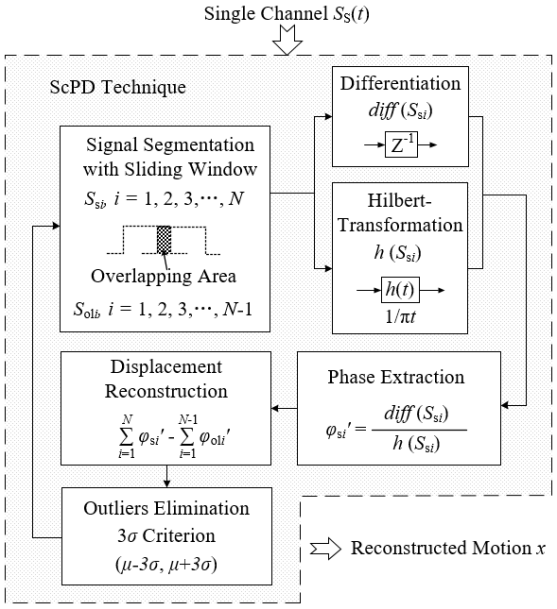

Fig. 3. Flowchart of the proposed ScPD technique with a single-channel signal. Steps: 1) signal segmentation using a sliding window; 2) signal processing based on differentiation and Hilbert transformation; 3) phase recreation via logical operation; and 4) signal smoothing based on the 3σ criterion.

the cell signal by differentiation. The differential process could be expressed as

$$S'_{si} = \phi'_i \cdot A_s \cos(\phi_i). \tag{5}$$

As (5) shows, there is a nonlinear term, $\cos(\phi_i)$, existing in the right side of the formula. To eliminate this nonlinear term, Hilbert transformation is utilized to reshape the window-cell signal S_{si}, which acts as a half-π phase shifter and implements a convolution to S_{si} with $1/\pi t$ in the time domain. Assume the target displacement varies less than $\lambda/4$ and meets the condition of the principle in (4). The cell signal S_{si} with the Hilbert transformation could be rewritten as

$$\widehat{S_{si}} = A_s \cos(\phi_i). \tag{6}$$

The desired phase in a single processing cell could be recreated by the first-order division with (5) and (6)

$$\phi'_i = \frac{S'_{si}}{\widehat{S_{si}}}. \tag{7}$$

Due to the restriction of the sampling rate of the ADC and the operating cost of the computer, endpoint distortion occurs in the signal shape with the Hilbert transformation. Overlapping areas with an equivalent length are designed between two observing window cells. Considering the differential form is vulnerable to noise, an integration step is introduced to cancel out noise distributions across zero axis. The digitized form of the reconstructed phase with the proposed ScPD technique could be expressed as follows:

$$\phi_i = \frac{\sum_{j=2}^{n} S_{si}[j] - S_{si}[j-1]}{H[S_{si}]} \tag{8}$$

$$\phi_{\mathrm{target}} = \sum_{i=1}^{N-1} \phi_i - \sum_{i=1}^{N-1} \phi_{\mathrm{ol}i} \tag{9}$$

Authorized licensed use limited to: Shanghai Jiaotong University. Downloaded on September 17,2023 at 14:27:56 UTC from IEEE Xplore. Restrictions apply.

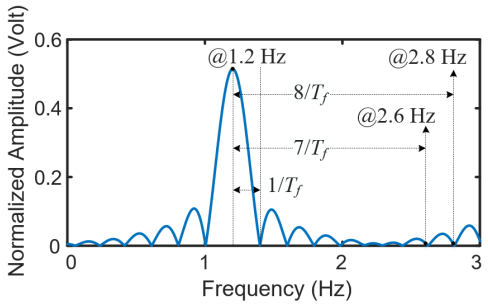

Fig. 4. Simulation results for the normalized spectrum of a 1.2-Hz sinusoidal motion detected by the custom-designed 120-GHz radar sensor system. The FFT window length, T_f, is set as 5 s.

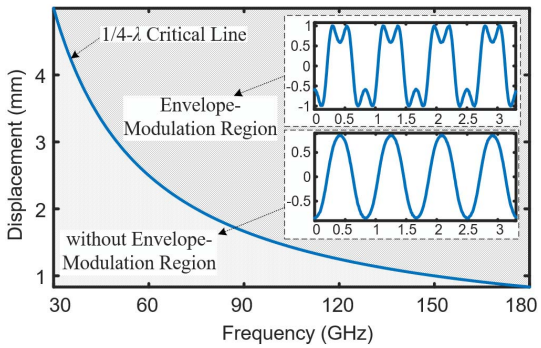

Fig. 5. The shape of the radar signal wave is related with the phase trajectory of the target motion. As Fig. 5 shows, the raw signal history may occur the envelope modulation which is aroused by the over 4-λ target motion displacement.

where ϕ_{oli} represents the reconstructed phase of the ith overlapping signal.

B. Optimization for Detection of Versatile Motions

The dc offsets of (1) and (2) are eliminated by simply estimating the mean power of the raw I/Q signals or filtered by the baseband with the ac-coupled architecture. The target motion is modulated in the phase of the backscattered signals, and the phase shift shows a relation to the traveling distance of the electromagnetic wave. When the object moves in the appropriate detecting area, the backscattered signals show an obvious variation to the moving displacement. On the contrary, when θ in the I/Q phases shows an integer multiple of π, the target moves in the null-point position, where the echoed phase is nonlinearly modulated and the output signal is buried in the baseline noise. The null-point signal may result in false demodulation and decrease the accuracy and robustness of the phase reconstruction. To avoid null-point errors, a selection strategy is developed by comparing the SNRs of the I/Q signals to pick the optimal channel for demodulation. As Fig. 4 shows, one of the quadrature signals modulated by a periodic motion at 1.2 Hz in phase is taken for an example, where T_f is the window length of the discrete Fourier transformation (DFT). To reduce the estimation errors aroused by the spectral leakage effect of DFT, a 7–8 times-of-$1/T_f$ frequency [21] interval is taken to calculate the baseline phase noise. The SNR of the signal as displayed in Fig. 4 is about 36 dB.

According to the small-angle approximation principle, the target motion with a displacement of less than $\lambda/4$ could be modeled as a linear motion and the signal trajectory will not happen in modulated envelope. However, for MMW radar interferometry, the carrier wavelength is ultrashort and subtle vibration may arouse ambiguity in the signal phase. For example, the $\lambda/4$-critical amplitude for a 120-GHz radar sensor is only 370 μm. By the method of the fast Fourier transformation (FFT) and inverse FFT (IFFT) transformation, an envelope extracting approach is developed to unwrap the modulated envelope of the selected single-channel signal. Moreover, as discussed in [22], the single-channel signal is comprised of infinite terms with Bessel-functions expansion. In the process of the continuous-to-discrete signal conversion, the sampling rate is difficult to meet the Nyquist theorem for the high-frequency parts of the signal, which may arouse endpoint jumping distortion [25] in the Hilbert transformation. To eliminate the endpoint effect and outliers, Pauta criterion [26] is leveraged to reject the abnormal values in the reconstructed phase, which adds more smoothness and stability of the recreated motion.

III. Simulation

Simulations are carried out based on a custom-designed 120-GHz interferometric radar to validate the proposed ScPD technique. All the motions are simulated with a frequency of 1.2 Hz. The sampling rate is set as 100 Hz.

A. Small-Displacement Motion Reconstruction

As discussed in the principle section, the backscattered signals show a relationship to the position of the moving target to be detected. As Fig. 6(a) illustrates, a sine motion with a frequency of 1.2 Hz and a displacement of 0.2 mm and SNR of 40 dB is simulated, of which the phase history length is only 2/25 λ at 120 GHz and the envelope shows no modulation. The phase trajectory is far less than $\lambda/4$ but sits across the first and second quadrants instead of in a single quadrant or across the first and fourth quadrants. In this situation, the extracted phase by the arctangent method occurs phase ambiguity and jumping truncation distortion in the recovered signal shape, as shown in Fig. 6(b). On the contrary, eliminating the I/Q calibration, the proposed ScPD technique recovers the displacement motion from a single channel without any phase ambiguity, which promotes a prominent accuracy to the reconstructed signal with a root mean square error (RMSE) of 0.002 mm, as shown in Fig. 6(c). The sliding window length is set as 0.2 s with a 0.01-s overlapping.

B. Signal-to-Noise Ratio Analysis

A motion with the same frequency and displacement as the discussed above is simulated. At this time, the target motion stays at the optimal detecting area for radar interferometry, but the motion is subjected to a poor SNR of 15 dB as well. The demodulated results with the arctangent method occur a lot of phase ambiguity, as shown in Fig. 7(a). Due to severe dependence on the accuracy of the I/Q calibration, the popular DACM algorithm loses effect on phase reconstruction and gets a false demodulation, as shown in Fig. 7(c). Although relaxing the requirement on the orthogonality of the I/Q signals, the signal history recovered by the arcsine algorithm loses much

Authorized licensed use limited to: Shanghai Jiaotong University. Downloaded on September 17,2023 at 14:27:56 UTC from IEEE Xplore. Restrictions apply.

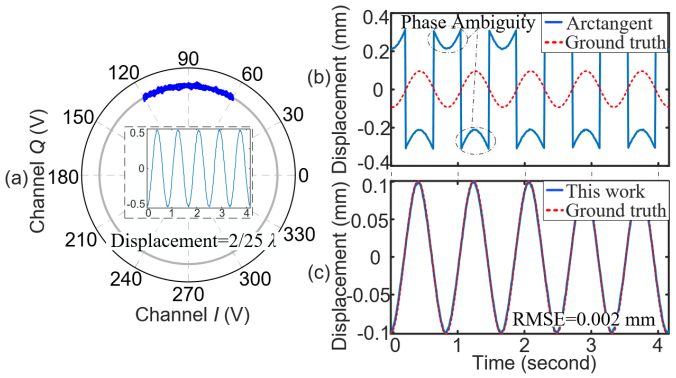

Fig. 6. Simulation results of a periodic motion suffering I/Q mismatch with a frequency of 1.2 Hz and a displacement of 0.2 mm (2/25 λ at 120 GHz, SNR: 40 dB). (a) Raw I/Q trajectory, and the recovered motion by (b) arctangent demodulation based on the quadrature signals from (a) with I/Q calibration, and (c) proposed ScPD technique with a single channel from (a) directly. The inset in (a) shows the selected single channel.

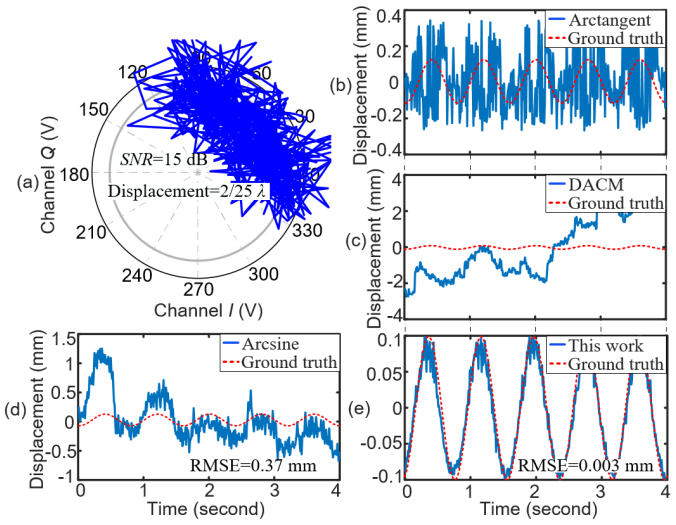

Fig. 7. Simulation results of a periodic motion suffering low SNR with a frequency of 1.2 Hz and a displacement of 0.2 mm (2/25 λ at 120 GHz, SNR: 15 dB). (a) Raw I/Q trajectory, and the recovered motions by (b) arctangent demodulation, (c) DACM algorithm, (d) arcsine algorithm with both the calibrated quadrature signals from (a), respectively, and (e) proposed ScPD technique with a single channel from (a) directly.

shape reality with an RMSE of 0.37 mm, as illustrated in Fig. 7(d). Unlike the conventional demodulations, a single channel is selected from Fig. 7(a) by the proposed ScPD technique and set the sliding-window length as 0.4 s and the overlapping as 0.03 s. Without the I/Q calibration, the reconstructed motion trajectory by the ScPD technique avoids the calibrating errors and performs a high tolerance to the poor SNR with an RMSE of 0.003 mm, which improves over 123 times than the arcsine algorithm, as shown in Fig. 7(e). A thorough comparison of the tolerance to SNR of the proposed ScPD technique and the state-of-the-art conventional demodulation methods is carried out, and the results are organized in the Appendix. More details could be referred to the Appendix [see Fig. 16(a)–(c) and Table II].

C. Large Displacement Motion Reconstruction

As discussed above, when the target displacement varies less than $\lambda/4$, the detected motion could be modeled as a linear function of t and will not arouse the phase ambiguity in the reconstructed motion trajectories. However, for the MMW radar interferometry, it is easier for the displacement motion to outstrip the $\lambda/4$ limitation, i.e., 0.625 mm for 120 GHz, and exhibit the envelope modulation in the I/Q signals. Based on the FFT and IFFT transformation, an envelope unwrapping approach is developed to improve the universality of the ScPD technique proposed in this work. As Fig. 8(a) shows, a periodic motion with a frequency of 1.2 Hz and a displacement of 1 mm (2/5 λ at 120 GHz, SNR: 40 dB) is simulated. The I/Q trajectory in the constellation diagram far outstrips $\lambda/4$ and the envelope of the single-channel signal is modulated. In this situation, the arctangent result, as shown in Fig. 8(b), occurs phase ambiguity because of the codomain limitation. On the contrary, the reconstructed motion histories with the DACM algorithm, the arcsine algorithm, and the proposed ScPD technique share a similar RMSE of about 0.009 mm, as shown in Fig. 8(c)–(e), respectively. The sliding window length is set as 0.2 s with a 0.01-s overlapping.

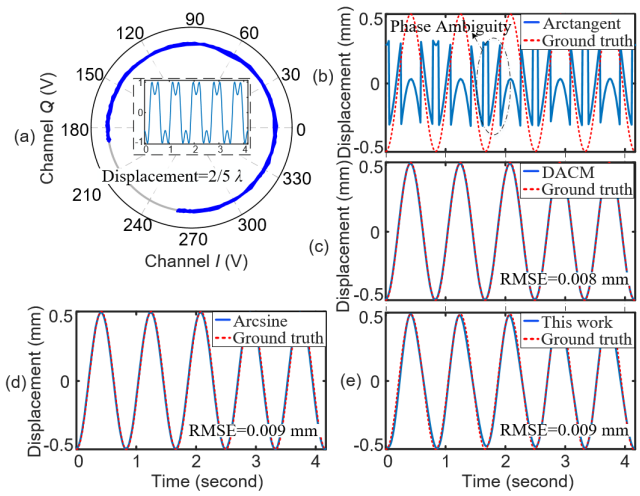

Fig. 8. Simulation results of a periodic motion suffering modulated envelope with a frequency of 1.2 Hz and a displacement of 1 mm (2/5 λ at 120 GHz, SNR: 40 dB). (a) Raw I/Q trajectory, and the recovered motions by (b) arctangent demodulation, (c) DACM algorithm, (d) arcsine algorithm based on the quadrature signals from (a) with I/Q calibration, respectively, and (e) proposed ScPD technique with a single channel from (a) directly. The inset in (a) shows the selected single channel.

D. I/Q Mismatch

Besides poor SNR, the conventional calibration step is also vulnerable to hardware drawbacks, such as I/Q mismatch. A sine motion with a frequency of 1.2 Hz and a displacement of 0.3 mm (3/25 λ at 120 GHz, SNR: 40 dB), which is subject to the I/Q mismatch, is simulated, as shown in Fig. 9(a). Although the target motion vibrates within the codomain limitation, the recovered signals with the arctangent method occur phase ambiguity because of mismatched I/Q signals, as shown in Fig. 9(b). Due to the severe dependence on the calibration accuracy and the I/Q orthogonality, both of the demodulating results with the DACM algorithm and the arcsine algorithm lose partial shape reality with RMSEs of 0.023 mm and 0.024 mm, as shown in Fig. 9(c) and (d), respectively. On the contrary, eliminating the calibrating errors aroused by the I/Q mismatch, the proposed ScPD technique unwraps the target phase from a single channel and optimizes

Authorized licensed use limited to: Shanghai Jiaotong University. Downloaded on September 17,2023 at 14:27:56 UTC from IEEE Xplore. Restrictions apply.

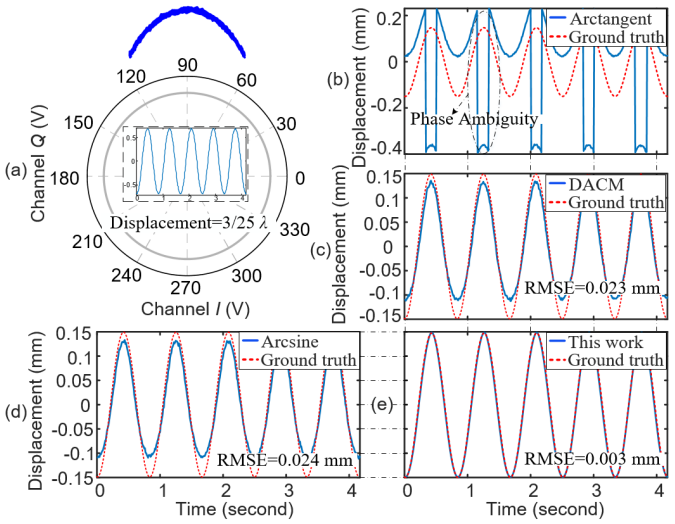

Fig. 9. Simulation results of a periodic motion suffering I/Q mismatch with a frequency of 1.2 Hz and a displacement of 0.3 mm (3/25 λ at 120 GHz, SNR: 40 dB). (a) Raw I/Q trajectory, and the recovered motions by (b) arctangent demodulation, (c) DACM algorithm, (d) arcsine algorithm based on the quadrature signals from (a) with I/Q calibration, respectively, and (e) proposed ScPD technique with a single channel from (a) directly. The inset in (a) shows the selected single channel.

the accuracy of the reconstructed signal history with an RMSE of 0.003 mm, which is almost eight times superior than conventional demodulations, as shown in Fig. 9(e). The sliding window length is set as 0.5 s with a 0.04-s overlapping. A thorough comparison of the tolerance to the I/Q mismatch of the proposed ScPD technique and the state-of-the-art conventional demodulation methods is carried out, and the results are organized in the Appendix. More details could be referred to the Appendix [see Fig. 1(a), (b), and (d) and Table III].

IV. Experiments

A custom-designed 120-GHz radar-sensor system is adopted to experimentally validate the proposed ScPD technique. A commercial 120-GHz radar transceiver (TRX_120_001@Silicon Radar), operational amplifiers (MAX9916EKA+@Maxim), and a low dropout regulator (LDO, MAX8902AATA+@Maxim) are selected to design the radar sensor system. The experimental setup is exhibited in Fig. 10. A linear-motor commercial actuator (X-LDM060C-AE54D12@Zaber) and a data acquisition device (USB-6001@NI) are selected. The sampling rate is set as 100 Hz.

A. Small-Displacement Motion Detection

As mentioned in Section III, the I/Q calibration processing is a necessary preceding step before the phase reconstruction by conventional demodulation methods. A CS technique, which works as an effective automatic calibration strategy to calibrate the quadrature I/Q signals, is introduced before the conventional demodulation processing in this article. The CS technique is developed from the LS method and optimizes the robustness and tolerance to noises and outliers, which greatly suppresses the errors aroused by false calibration. All the traditional demodulations exhibited in this article are implemented on the basis of the CS calibration.

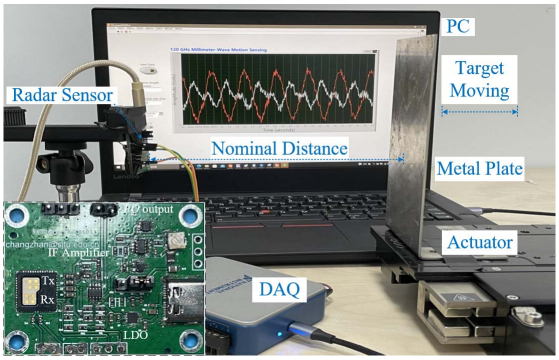

Fig. 10. Experimental setup of noncontact motion sensing with the custom designed 120-GHz interferometric radar sensor. The inset is the photograph of the custom-designed 120-GHz radar sensor.

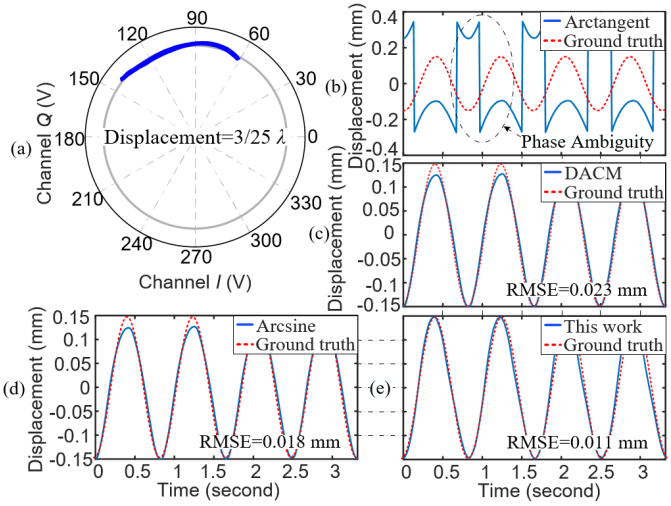

Fig. 11. Experimental results of a periodic motion with a frequency of 1.2 Hz and a displacement of 0.3 mm (3/25 λ at 120 GHz). (a) Raw I/Q trajectory, and the recovered motions by (b) arctangent demodulation, (c) DACM algorithm, (d) arcsine algorithm based on the quadrature signals from (a) with I/Q calibration, respectively, and (e) proposed ScPD technique with a single channel from (a) directly.

A metal plate is fixed on an actuator, which is programmed to take a sinusoidal motion with a frequency of 1.2 Hz and a displacement of 0.3 mm (3/25 λ at 120 GHz) at a nominal distance of 200 mm from the radar sensor. It is seen from Fig. 11(a) that the raw I/Q trajectory undergoes a little distortion. In this situation, although the target displacement vibrates within the codomain limitation, the recreated motion with the arctangent method still occurs phase ambiguity in wave history, as shown in Fig. 11(b). In contrast, both the DACM and arcsine algorithms solve the phase ambiguity problem, while their demodulation results displace shape distortions aroused by unmatched phase balance with RMSEs of 0.023 and 0.018 mm, as shown in Fig. 11(c) and (d), respectively. Only involving a single channel, the proposed ScPD technique gets rid of the calibrating process and relaxes the dependence on quadrature balance, which avoids false calibration induced errors effectively and optimizes the reconstructed motion with an RMSE of 0.11 mm, nearly half of the conventional results, as shown in Fig. 11(e). The sliding window length is set as 0.5 s and the overlapping is 0.03 s.

Authorized licensed use limited to: Shanghai Jiaotong University. Downloaded on September 17,2023 at 14:27:56 UTC from IEEE Xplore. Restrictions apply.

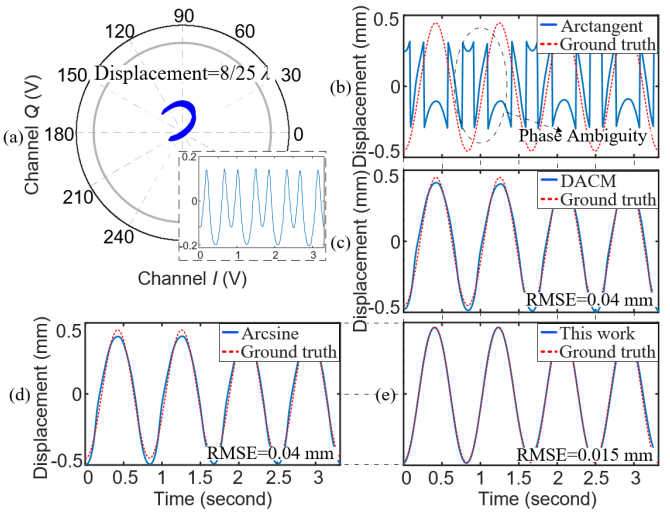

Fig. 12. Experimental results of a periodic motion with a frequency of 1.2 Hz and a displacement of 0.8 mm (8/25 λ at 120 GHz). (a) Raw I/Q trajectory, and the recovered motions by (b) arctangent demodulation, (c) DACM algorithm, (d) arcsine algorithm based on the quadrature signals from (a) with I/Q calibration, respectively, and (e) the proposed ScPD technique with a single channel from (a) directly. The inset in (a) shows the selected single channel.

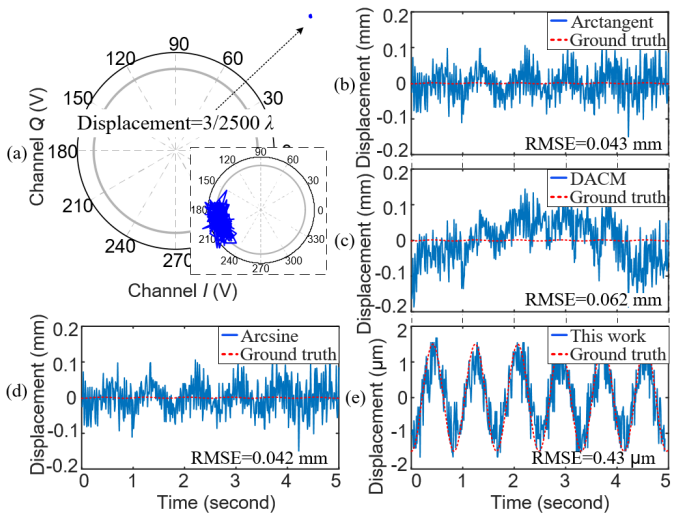

Fig. 13. Experimental results of a periodic motion with a frequency of 1.2 Hz and a displacement of 3 μm (3/2500 λ at 120 GHz). (a) Raw I/Q trajectory, and the recovered motions by (b) arctangent demodulation, (c) DACM algorithm, (d) arcsine algorithm based on the quadrature signals from (a) with I/Q calibration, respectively, and (e) proposed ScPD technique with a single-channel signal from (a) directly. The inset shows the calibrated I/Q trajectory by the CS technique.

B. Large-Displacement Motion Detection

By unwrapping the signal envelope, the proposed ScPD technique could succeed in recovering the target motion with a displacement over $\lambda/4$. The actuator is programmed to take a sinusoidal motion with a frequency of 1.2 Hz and a displacement of 0.8 mm (8/25 λ at 120 GHz) at a nominal distance of 200 mm. It is seen from Fig. 12(a) that the raw signal suffers a modulated envelope. Due to outstripping the codomain limitation, the demodulated result with the arctangent method shows a phase ambiguity, as shown in Fig. 12(b). Although the phase reconstruction process with the DACM and the arcsine algorithms get rid of the codomain limitation, the recovered motion histories lose partial shape realities and show the accuracy with the same RMSE of 0.04 mm, as shown in Fig. 12(c) and (d), respectively. It is because the modulated envelopes hinder the phase-center estimation, which leads to the incorrect I/Q calibration and adds the demodulation errors. Canceling the I/Q calibrating step, the proposed ScPD technique reconstructs the target motion from a single channel and the recreated motion trajectory shows an RMSE of 0.015 mm, which is almost three times better than the conventional demodulations, as shown in Fig. 12(d). The sliding window length is set as 0.5 s and the overlapping is 0.07 s.

C. Subtle Vibration Detection

The proposed ScPD technique is superior in deep subwavelength motion detection. The metal plate moving with the actuator is taking a periodic motion with a frequency of 1.2 Hz and a displacement of 3 μm (3/2500 λ at 120 GHz). As shown in Fig. 13(a), the raw I/Q trajectory is a "point" beyond the unit phase circle. In this situation, the I/Q arc is too short to supply the sufficient phase information to get the accurate fitting center, which makes the I/Q calibration fail and results in the false demodulations. Although the arctangent and the arcsine methods are expert in tackling the motion reconstruction with the displacements within the range of $(-\pi/2, \pi/2)$, only the period of the motion in the time domain could be observed in the recovered results by the two methods, but wrong displacements are achieved with similar RMSEs of 0.043 and 0.042 mm, as shown in Fig. 13(b) and (d), respectively. It is because the precalibration process is unable to determine the precise fitting radius and even a length ambiguity takes place in the I/Q trajectory due to the false calibration. As Fig. 13(c) exhibits, the recovered trajectory with the DACM algorithm loses the reality of both the frequency and amplitude with an RMSE of 0.062 mm, which shows the least robustness and tolerance to calibration errors among the three conventional methods. On the contrary, the proposed ScPD technique still works well and the reconstructed motion shows similar a trajectory to the ground truth with an RMSE of 0.43 μm. The sliding window length is set as 0.5 s and the overlapping is 0.01 s.

D. Microgesture Detection

Besides the regular periodic motion, the proposed ScPD technique also has an advantage in irregular motion detection, such as the microgesture recognizing. As shown in Fig. 14(a), the thumb snaps randomly in the nominal distance of 150 mm in front of the radar sensor. It is seen from Fig. 14(b) that the single-channel signal wave of finger snapping shows inconstant displacements and the uncertain period. With the proposed ScPD technique, the snapping-gesture trajectory could be reconstructed accurately, as shown in Fig. 14(c). The sliding window length is set as 0.4 s and the overlapping is 0.02 s.

E. Vital Sign Monitoring

Moreover, the proposed ScPD technique could be adopted to monitor the respiratory frequency and the heart rate. A person

Authorized licensed use limited to: Shanghai Jiaotong University. Downloaded on September 17,2023 at 14:27:56 UTC from IEEE Xplore. Restrictions apply.

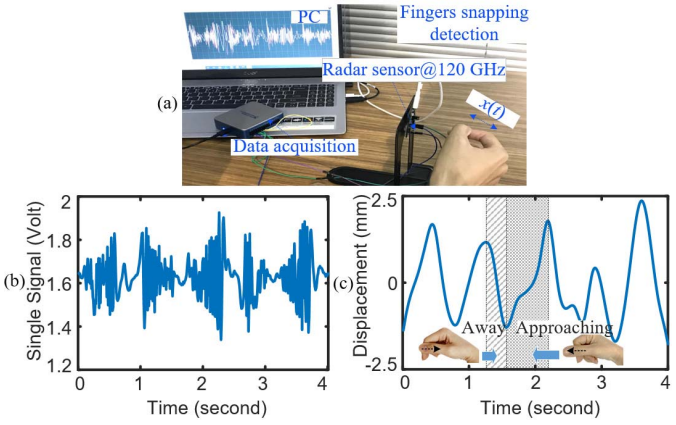

Fig. 14. Experimental results of microgesture-fingers snapping within 5 mm (2 λ at 120 GHz). (a) Experimental setup. (b) Raw data of the selected single channel with the proposed ScPD technique. (c) Gesture motion recreated by the demodulation system proposed in this article.

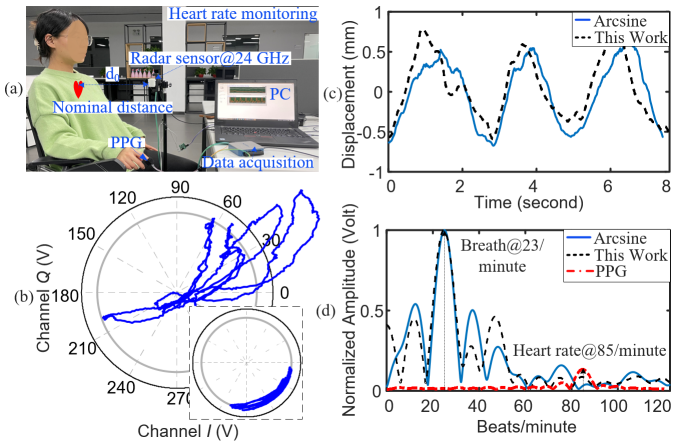

Fig. 15. Experimental results of vital sign monitoring within 1.5 mm (3/25 λ at 24 GHz). (a) Experimental setup. (b) Raw I/Q trajectory. (c) Chest-wall movements recreated by the arcsine algorithm and the proposed ScPD technique. (d) Breathe frequency and the heart rate from the demodulation results in (c) and the heart rate detected by PPG device. The inset shows the compensated I/Q trajectory by signal preconditioning methods.

sits in front of the radar sensor at a nominal distance of 350 mm, as shown in Fig. 15(a). As a control group, the photo plethysmography (PPG) device is clamped on the index finger of the right hand to detect the pulse rate. It is seen from Fig. 15(b) that the raw I/Q trajectory exhibits a shape distortion, such as the ribbon distortion aroused by the ac-coupling architecture. That means, it is necessary to add preconditioning steps, such as ac-coupling induced error correction [27], the dc offsets calibration [7], and the I/Q mismatch correction [28] to compensate the distortion before the traditional demodulation processes. As shown in Fig. 15(c), the chest-wall movement recreated with the proposed ScPD technique based on a raw channel shares a similar wave history with the arcsine algorithm based on the well-compensated orthogonal signals. The sliding window length is set as 0.5 s and the overlapping is 0.09 s. The respiratory rates of both the two demodulations in Fig. 15(c) are overlapped of 23 breaths/min, but the reconstructed result with the proposed ScPD technique shows a heart rate of 85 beats/min as the same as the PPG result, as shown in Fig. 15(d).

TABLE I
PERFORMANCE COMPARISON: SCPD VERSUS THE STATE-OF-THE-ART METHODS

Key demodulation method	RMSE of recreated results/mm	Running time/s
Arctangent	0.14	0.75
DACM	0.18	1.93
Arcsine	0.18	6.77
This work	0.14	0.29

V. DISCUSSION

To implement a through comparison of the proposed ScPD technique with other alternative state-of-the-art demodulation methods, a custom-designed 120-GHz radar-sensor system is adopted for the motion interferometry and the actuator is programmed to move sinusoidally with a frequency of 1.2 Hz and a displacement of 0.3 mm (3/25 λ at 120 GHz) at a nominal distance of 200 mm. The experimental setup is exhibited in Fig. 6. The sampling rate of the data acquisition is 100 Hz and the observation time is 80 s. Multiple preconditioning steps, including ac coupling induced distortion correction, I/Q mismatch correction, and dc offsets calibration, are introduced before the motion reconstruction with the traditional demodulation methods. As Table I shows, the RMSE of the recovered motion by the proposed ScPD technique based on a raw channel is the same as that of the arctangent result based on the well-compensated orthogonal signals, which is superior to the results by the DACM and the arcsine demodulation. To demonstrate the computational efficiency, the running time of the entire process from inputting the raw signals to achieve the reconstructed motion is estimated. It is obviously seen that the time of the whole process of reconstructing the motion by this work is only 0.29 s, which is 2.6 times faster than the arctangent demodulation, 6.7 times than the DACM method, and over 23 times than the arcsine method.

VI. CONCLUSION

An ScPD technique is proposed for accurate motion sensing using interferometric radar. To tackle various motions with regular and irregular patterns, several processing steps including null point rejection, envelope unwrapping, and outlier elimination are introduced with the ScPD technique. A series of simulations and experiments are carried out to validate the proposed technique. Compared with the conventional demodulations, the proposed ScPD technique in this article only involves one single receiver channel, instead of bothering the quadrature I/Q architecture. Moreover, it eliminates the signal calibration step, which not only simplifies the demodulation process but also avoids the errors aroused by false calibration and improves the accuracy of the motion reconstruction.

Authorized licensed use limited to: Shanghai Jiaotong University. Downloaded on September 17,2023 at 14:27:56 UTC from IEEE Xplore. Restrictions apply.

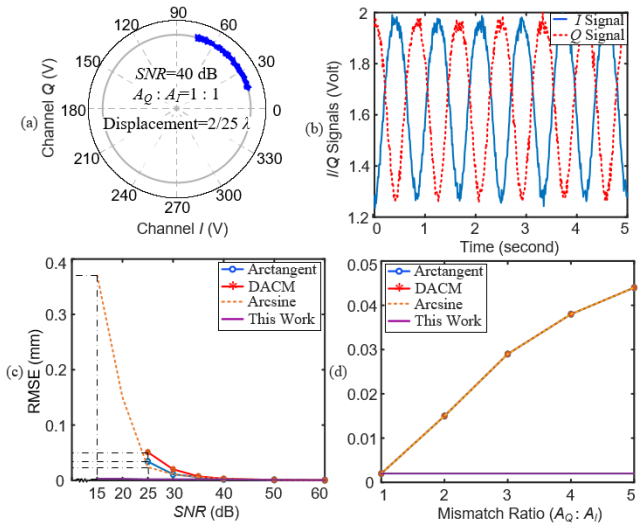

Fig. 16. Simulation results of a periodic motion suffering various SNR with a frequency of 1.2 Hz and a displacement of 0.2 mm (2/25 λ at 120 GHz). (a) Raw I/Q trajectory and (b) corresponding I/Q signals with the SNR of 40 dB and a mismatch ratio of 1:1 for example, and the comparison results of (c) SNR tolerances of the various demodulation methods with the variation of the SNR from 15 to 60 dB, and (d) tolerance to the I/Q mismatch by various demodulation methods with the mismatch ratio from 1 to 5, respectively.

APPENDIX

To verify the tolerance to SNR of the proposed ScPD technique, a series of sinusoidal motions with a frequency of 1.2 Hz and a displacement of 0.2 mm (2/25 λ at 120 GHz) suffering various SNR are simulated. As the Appendix [Fig. 16(a)] shows, the raw I/Q trajectory sits on the unit phase circle in a single quadrant and the mismatch ratio (A_Q/A_I, A_I and A_Q represent the amplitudes of the I/Q signals, respectively) of the I/Q signals is 1:1. That said, the I/Q phases vary within the codomain limitation of $(-\pi/2, \pi/2)$ to the arctangent demodulation, which eliminates the impact of the phase ambiguity on the simulation results. Both the arctangent demodulation and the DACM method make sense on the motion reconstruction in the SNR better than 25-dB situation, while the phase recreation of motion with the SNR of 15 dB by the arcsine method and the proposed ScPD technique shows an accuracy with an RMSE of 0.37 and 0.003 mm, respectively, as shown in the Appendix [see Fig. 16(c)]. Within the SNR range of 15–60 dB, the motion reconstruction by this work shows superior to tackle the SNR issue with a stable RMSE within (0.003–0.0004 mm). The sliding window length is set as 0.5 s with an overlapping of 0.03 s for all simulations. Besides, with the SNR increasing, the simulated results by different methods show a similar RMSE of 0.0004 mm at last. The detailed experimental results are organized in the Appendix (see Table II).

A series of sinusoidal motions with a frequency of 1.2 Hz and a displacement of 0.2 mm (2/25 λ at 120 GHz) under the various I/Q mismatch ratios are simulated. The SNR of the I/Q signals is fixed as 40 dB. It is seen from the Appendix [see Fig. 16(d)] that the RMSEs of the reconstruction results by the arctangent method, the DACM algorithm, and the arcsine technique share a similar variation tendency, while the proposed ScPD technique recovers the target motions suffering the I/Q mismatch ratio from 1 to 5 with a demodulation accuracy with a stable RMSE of 0.002 mm. The sliding window length is set as 0.5 s with an overlapping of 0.03 s for all simulations. The detailed experimental results are organized in the Appendix (see Table III).

TABLE II
TOLERANCE TO SNR: SCPD VERSUS THE STATE-OF-THE-ART METHODS

RMSE/mm SNR/dB	MA	MB	MC	MD
15	-	-	0.37	0.003
20	-	-	0.15	0.003
25	0.034	0.051	0.024	0.002
30	0.011	0.02	0.011	0.002
35	0.006	0.008	0.006	0.002
40	0.002	0.003	0.003	0.002
50	0.001	0.001	0.001	0.001
60	0.0004	0.0004	0.0004	0.0004

(MA: arctangent technique; MB: DACM technique; MC: arcsine technique; MD: the proposed ScPD technique.)

TABLE III
TOLERANCE TO I/Q MISMATCH: SCPD VERSUS THE STATE-OF-THE-ART METHODS

RMSE/mm $A_Q : A_I$	MA	MB	MC	MD
1	0.002	0.003	0.003	0.002
2	0.015	0.015	0.015	0.002
3	0.029	0.029	0.029	0.002
4	0.038	0.038	0.038	0.002
5	0.044	0.044	0.044	0.002

(MA: arctangent technique; MB: DACM technique; MC: arcsine technique; MD: the proposed ScPD technique.)

REFERENCES

[1] Y. Luo, H. Song, R. Y. Wang Deng, F. Zhao, and Z. Xu, "Arc FMCW SAR and applications in ground monitoring," *IEEE Trans. Geosci. Remote Sens.*, vol. 52, no. 9, pp. 5989–5998, Sep. 2014.
[2] Y. Gao and R. Zoughi, "Millimeter wave reflectometry and imaging for noninvasive diagnosis of skin burn injuries," *IEEE Trans. Instrum. Meas.*, vol. 66, no. 1, pp. 77–84, Jan. 2017.
[3] C. Li et al., "A review on recent progress of portable short-range noncontact microwave radar systems," *IEEE Trans. Microw. Theory Techn.*, vol. 65, no. 5, pp. 1692–1706, May 2017.
[4] Y. Zhang, J. Li, S. Wei, F. Zhou, and D. Li, "Heartbeats classification using hybrid time-frequency analysis and transfer learning based on ResNet," *IEEE J. Biomed. Health Informat.*, vol. 25, no. 11, pp. 4175–4184, Nov. 2021.
[5] S. Mann et al., "High-precision interferometric radar for sheet thickness monitoring," *IEEE Trans. Microw. Theory Techn.*, vol. 66, no. 6, pp. 3153–3166, Jun. 2018.
[6] H. Zhang, J. Liang, and Z. Zhang, "Active fault tolerant control of adaptive cruise control system considering vehicle-borne millimeter wave radar sensor failure," *IEEE Access*, vol. 8, pp. 11228–11240, 2020.
[7] S. Linz, F. Lurz, R. Weigel, and A. Koelpin, "A review on six-port radar and its calibration techniques," in *Proc. 22nd Int. Microw. Radar Conf. (MIKON)*, Poznań, Poland, May 2018, pp. 80–83.
[8] S. Li, Y. Xiong, Z. Ren, C. Gu, and Z. Peng, "Ultra-micro vibration measurement method using CW Doppler radar," in *Proc. Int. Conf. Sens., Meas. Data Anal. Era Artif. Intell. (ICSMD)*, Oct. 2020, pp. 235–237.
[9] W. Xu, C. Gu, C. Li, and M. Sarrafzadeh, "Robust Doppler radar demodulation via compressed sensing," *Electron. Lett.*, vol. 48, no. 22, pp. 1428–1430, Oct. 2012.
[10] K. Staszek, S. Linz, F. Lurz, S. Mann, R. Weigel, and A. Koelpin, "Improved calibration procedure for six-port based precise displacement measurements," in *Proc. IEEE Top. Conf. Wireless Sensors Sensor Netw. (WiSNet)*, Jan. 2016, pp. 60–63.

Authorized licensed use limited to: Shanghai Jiaotong University. Downloaded on September 17,2023 at 14:27:56 UTC from IEEE Xplore. Restrictions apply.

[11] H. Deng, G. Farquharson, J. Sahr, Y. Goncharenko, and J. Mower, "Phase calibration of an along-track interferometric FMCW SAR," *IEEE Trans. Geosci. Remote Sens.*, vol. 56, no. 8, pp. 4876–4886, Aug. 2018.
[12] X. Gao and O. Boric-Lubecke, "Radius correction technique for Doppler radar noncontact periodic displacement measurement," *IEEE Trans. Microw. Theory Techn.*, vol. 65, no. 2, pp. 621–631, Feb. 2017.
[13] L. Zhang et al., "Kalman filter and cross-multiply algorithm with adaptive DC offset removal," *IEEE Trans. Instrum. Meas.*, vol. 71, pp. 1–10, 2022.
[14] C. Will et al., "Segmental polynomial approximation based phase error correction for precise near field displacement measurements using six-port microwave interferometers," in *Proc. IEEE Top. Conf. Wireless Sensors Sensor Netw. (WiSNet)*, Jan. 2017, pp. 23–25.
[15] W. Xu, C. Gu, and J.-F. Mao, "Deep sub-wavelength millimeter-wave radar interferometry with a novel ego-motion based calibration technique," in *IEEE MTT-S Int. Microw. Symp. Dig.*, Jun. 2021, pp. 282–285.
[16] S. Linz et al., "I/Q imbalance compensation for six-port interferometers in radar applications," in *Proc. 44th Eur. Microw. Conf.*, Oct. 2014, pp. 746–749.
[17] J. Park et al., "Polyphase-basis discrete cosine transform for real-time measurement of heart rate with CW Doppler radar," *IEEE Trans. Microw. Theory Techn.*, vol. 66, no. 3, pp. 1644–1659, Mar. 2018.
[18] W. Xu, Y. Li, C. Gu, and J.-F. Mao, "Large displacement motion interferometry with modified differentiate and cross-multiply technique," *IEEE Trans. Microw. Theory Techn.*, vol. 69, no. 11, pp. 4879–4890, Nov. 2021.
[19] J. Wang, X. Wang, L. Chen, J. Huangfu, C. Li, and L. Ran, "Noncontact distance and amplitude-independent vibration measurement based on an extended DACM algorithm," *IEEE Trans. Instrum. Meas.*, vol. 63, no. 1, pp. 145–153, Jan. 2014.
[20] Q. Lv et al., "High dynamic-range motion imaging based on linearized Doppler radar sensor," *IEEE Trans. Microw. Theory Techn.*, vol. 62, no. 9, pp. 1837–1846, Sep. 2014.
[21] T. Fan et al., "Wireless hand gesture recognition based on continuous-wave Doppler radar sensors," *IEEE Trans. Microw. Theory Techn.*, vol. 64, no. 11, pp. 4012–4020, Nov. 2016.
[22] W. Xu, C. Gu, and J. Mao, "Interferometric motion sensing with a single-channel radar sensor based on a novel calibration-free phase demodulation technique," *IEEE Microw. Wireless Compon. Lett.*, vol. 32, no. 6, pp. 807–810, Jun. 2022.
[23] J. Liu, C. Gu, and J. Mao, "DC-independent high-linear motion sensing based on a novel ACAA algorithm," *IEEE Microw. Wireless Compon. Lett.*, vol. 32, no. 3, pp. 261–264, Mar. 2022.
[24] C. Gu and C. Li, "Frequency-selective distortion in continuous-wave radar displacement sensor," *Electron. Lett.*, vol. 48, no. 23, pp. 1495–1497, Nov. 2012.
[25] P. Li, J. Gao, D. Xu, C. Wang, and X. Yang, "Hilbert–Huang transform with adaptive waveform matching extension and its application in power quality disturbance detection for microgrid," *J. Mod. Power Syst. Clean Energy*, vol. 4, no. 1, pp. 19–27, Jan. 2016.
[26] J. Ding and J. Cai, "Two-side coalitional matching approach for joint MIMO-NOMA clustering and BS selection in multi-cell MIMO-NOMA systems," *IEEE Trans. Wireless Commun.*, vol. 19, no. 3, pp. 2006–2021, Mar. 2020.
[27] C. Gu, Z. Peng, and C. Li, "High-precision motion detection using low-complexity Doppler radar with digital post-distortion technique," *IEEE Trans. Microw. Theory Techn.*, vol. 64, no. 3, pp. 961–971, Mar. 2016.
[28] D. Rodriguez and C. Li, "Sensitivity and distortion analysis of a 125-GHz interferometry radar for submicrometer motion sensing applications," *IEEE Trans. Microw. Theory Techn.*, vol. 67, no. 12, pp. 5384–5395, Dec. 2019.

Wei Xu (Graduate Student Member, IEEE) received the B.S. degree in electronic science and technology from Zhejiang University, Hangzhou, China, in 2016, and the M.S. degree in radio physics from the China Academy of Engineering Physics, Beijing, China, in 2019. She is currently pursuing the Ph.D. degree in electronic engineering at Shanghai Jiao Tong University, Shanghai, China.

Her research interests include analog/RF systems and the interferometric millimeter-wave radar sensing technologies.

Shuqin Dong (Graduate Student Member, IEEE) received the B.S. degree in electronic and information Engineering from Xidian University, Xi'an, China, in 2017, and the M.S. degree in electronic science and technology from Zhejiang University, Hangzhou, China, in 2020. She is currently pursuing the Ph.D. degree in electronic and information at Shanghai Jiao Tong University, Shanghai, China.

From 2020 to 2021, she was a Software Algorithm Engineer with Huawei Technologies, Shenzhen, China. Her research interests include biomedical radar, health informatics, and signal processing.

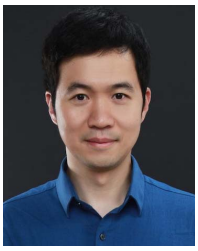

Changzhan Gu (Senior Member, IEEE) received the B.S. and M.S. degrees from Zhejiang University, Hangzhou, China, in 2006 and 2008, respectively, the M.S. degree from the University of Florida, Gainesville, FL, USA, in 2010, and the Ph.D. degree in electrical engineering from Texas Tech University, Lubbock, TX, USA, in 2013.

Before returning to academia, he was with Google, Mountain View, CA, USA, where he was involved in the research and development of millimeter-wave gesture radar technology and translating it into consumer products. He is currently an Associate Professor with Shanghai Jiao Tong University, Shanghai, China.

Dr. Gu is a member of the IEEE MTT-S TC28 and the Secretary of MTT-S Shanghai Chapter. He received nine times' Best/Excellent Paper Awards from IEEE conferences as an author/coauthor. He received the IEEE Sensors Council Early Career Technical Achievement Award in 2019, the Okawa Foundation Research Grant in 2019, and the IEEE MTT-S Graduate Fellowship in Medical Applications in 2013. He is the TPC Chair for the 2022 IEEE International Microwave Biomedical Conference (IMBioC). He served on multiple technical subcommittees for the IEEE International Microwave Symposium (IMS) from 2018 to 2022. He was an Associate Editor of the IEEE TRANSACTIONS ON BIOMEDICAL CIRCUITS AND SYSTEMS (TBioCAS) from 2019 to 2021, an Area Editor of the *International Journal of Electronics and Communications* from 2014 to 2016, and a Guest Editor of the IEEE TRANSACTIONS ON MICROWAVE THEORY AND TECHNIQUES (TMTT) Special Issue on RWW2022. He is an Associate Editor of the IEEE JOURNAL OF ELECTROMAGNETICS, RF AND MICROWAVES IN MEDICINE AND BIOLOGY (J-ERM) and the *IET Microwave, Antenna and Propagation* (MAP).

Junfa Mao (Fellow, IEEE) received the B.S. degree in radiation physics from the National University of Defense Technology, Changsha, China, in 1985, the M.S. degree in experimental nuclear physics from the Shanghai Institute of Nuclear Research, Chinese Academy of Sciences, Beijing, China, in 1988, and the Ph.D. degree in electronic engineering from Shanghai Jiao Tong University (SJTU), Shanghai, China, in 1992.

Since 1992, he has been a Faculty Member with SJTU, where he is currently a Chair Professor. He is also an Academician of the Chinese Academy of Sciences. He has authored or coauthored more than 250 journal articles (including more than 110 IEEE journal articles) and 140 international conference papers.

Dr. Mao is a member of the Chinese Academy of Sciences. He was a member of the 2012–2014 IEEE Microwave Theory and Techniques Society Fellow Evaluation Committee and the 2015 IEEE Fellow Committee, and the Founder and the 2007–2009 Chair for the IEEE Shanghai Section. He is a Fellow of the China Institute of Electronics (CIE). He received the National Natural Science Award of China in 2004, the National Technology Invention Award of China in 2008, the National Science and Technology Advancement Award of China in 2012, ten best paper awards of international conferences, and two National Awards of Teaching in 2005 and 2018. He is a Chief Scientist of the National Basic Research Program (973 Program) of China, a Project Leader of the Natural Science Foundation of China for Creative Research Groups, a Cheung Kong Scholar of the Ministry of Education, China, the Director of the Microwave Society of CIE, and the 2009–2019 Chair for the IEEE MTT-S Shanghai Chapter.

Authorized licensed use limited to: Shanghai Jiaotong University. Downloaded on September 17,2023 at 14:27:56 UTC from IEEE Xplore. Restrictions apply.